Chemical Physics Letters 586 (2013) 153–158

Contents lists available at ScienceDirect

Chemical Physics Letters

journal homepage: www.elsevier.com/locate/cplett

Quantum chemical calculation of intramolecular vibrational redistribution and vibrational energy transfer of water clusters

Y.L. Niu [a], R. Pang [a,b], C.Y. Zhu [a,*], M. Hayashi [c], Y. Fujimura [d], S.H. Lin [a,d,*], Y.R. Shen [e]

[a] Department of Applied Chemistry, Institute of Molecular Science and Center for Interdisciplinary Molecular Science, National Chiao Tung University, Hsinchu, Taiwan, ROC
[b] State Key Laboratory of Physical Chemistry of Solid Surfaces, and College of Chemistry and Chemical Engineering and Xiamen University, Xiamen 361005, Fujian, PR China
[c] Center for Condensed Matter Sciences, National Taiwan University, Taipei, Taiwan, ROC
[d] Institute of Atomic and Molecular Sciences (IAMS), Academia Sinica, Taipei, Taiwan, ROC
[e] Department of Physics, University of California, Berkeley, CA, USA

ARTICLE INFO

Article history:
Received 18 March 2013
In final form 5 September 2013
Available online 13 September 2013

ABSTRACT

In present letter the adiabatic approximation is applied to the intramolecular vibrational redistribution (IVR) of water clusters. The isotope, blocking and cluster-size effects are investigated. This letter also examines the assumption associated with the transition state theory applied to unimolecular reactions; that is, IVR is assumed to be completed before the reaction takes place. For this purpose, we choose to study $(H_2O)_2H^+ \rightarrow H_2O + H_3O^+$, and $(H_2O)_2 \rightarrow 2H_2O$ processes. In molecular clusters, the vibrational excitation energy transfer between different normal modes has been observed. This will also be investigated for the deuterated species of $(HOD)_2H^+$.

1. Introduction

Recently experimental [1–7] and theoretical [8–16] investigations of the vibrational redistribution dynamics of water and other molecules in condensed phases have attracted a considerable attention. Hynes and co-workers studied the vibrational redistribution of OH stretch excitations to bending to librational degrees of freedom in water liquid in linear coupling model [15]. Skinner and co-workers discussed the validity of Förster theory model for the vibrational energy transfer in water liquid [13]. Bowman and co-workers simulated the predissociation of water dimers and discuss the process of energy flow from bond stretching to the bond bending [17]. In comparison the first principle calculation of the vibrational redistribution dynamics of isolated molecules has received much less attention [18–20]. A theoretical approach based on the adiabatic approximation model of vibrational redistribution has been developed [8,12]. In this Letter, we shall present its application to the vibrational dynamics of water clusters $(H_2O)_n$ and $(H_2O)_nH^+$, where $n = 2$, 3, 4, and their isotope species. The RRKM (Rice–Ramsperger–Kassel–Marcus) theory is a very popular and well received theory applied to treat the unimolecular reactions of isolated (i.e., collision-free) molecules and clusters [21–24]. Lin and et al. have recently applied Morse potential model to develop the anharmonic RRKM theory [25–28]. Fundamentally it is based on the transition state theory which assumes that intramolecular vibrational redistribution (IVR) is much faster than unimolecular reactions so that the vibrational equilibrium is established before the reaction takes place. IVR plays an important role not only in unimolecular reactions but also in photochemistry and photophysics. Due to the fact that in the harmonic oscillator approximation when a vibrational mode is excited the excitation energy will be localized in that mode and will not flow into other modes, for IVR to take place, the anharmonic potential energy function which describes the coupling among different modes is needed. This information has become available only recently in the quantum chemistry programs and will be employed to perform the calculation of IVR in this Letter [29,30].

In treating the unimolecular decomposition of molecular clusters by using the RRKM theory the anharmonic effect is very important and it has been recently included in the conventional RRKM theory. This has been applied to study the decomposition of $(H_2O)_2$, $((H_2O)_2 \rightarrow 2H_2O)$ [27] and $(H_2O)_2H^+$, $((H_2O)_2H^+ \rightarrow (H_2O)H^+ + H_2O)$ [25]. For the purpose of the investigation of the effect of IVR on the RRKM theory, we shall calculate the IVR of $(H_2O)_2$ and $(H_2O)_2H^+$ and compare these IVR rates with the anharmonic decomposition rates of these clusters. This can then be used to examine the validity of the RRKM theory applied to these clusters.

In molecular clusters, the vibrational excitation energy transfer from one mode to another has been observed. This will also be investigated in the deuterated species of $(HOD)_2H^+$.

The present letter is organized as follows. Following the introduction, a brief theory of IVR will be presented in Section 2, which

* Corresponding authors at: Department of Applied Chemistry, Institute of Molecular Science and Center for Interdisciplinary Molecular Science, National Chiao Tung University, Hsinchu, Taiwan, ROC.

E-mail addresses: cyzhu@mail.nctu.edu.tw (C.Y. Zhu), sheng@mail.nctu.edu.tw (S.H. Lin).

0009-2614/$ - see front matter © 2013 Elsevier B.V. All rights reserved.
http://dx.doi.org/10.1016/j.cplett.2013.09.019

will be followed by the presentation of the calculated results of IVR of $(H_2O)_2$, $(H_2O)_2H^+$ and the deuterated species of $(H_2O)_2H^+$ in Section 3. The discussion of vibrational energy transfer within $(HOD)_2$-H^+, and the validity of RRKM method on $(H_2O)_2$ and $(H_2O)_2H^+$ will be given in Section 4. Then a brief summary will be given in Section 5.

2. Theory of IVR

We consider the adiabatic approximation model for isolated molecules or clusters, which is similar to the Born–Oppenheimer approximation model for molecules; that is, electronic coordinates corresponds to high frequency normal coordinates $\{Q_I\}$, nuclear coordinates corresponds to low frequency normal coordinates $\{q_i\}$, UV–visible spectra corresponds to IR vibrational spectra and internal conversion corresponds to IVR. It follows that to solve

$$H\Psi_{av}(\mathbf{Q},\mathbf{q}) = E_{av}\Psi_{av}(\mathbf{Q},\mathbf{q}) \tag{1}$$

where

$$H = T_L + T_H + V = T_L + H_H \tag{2}$$

is the total vibrational Hamiltonian, and

$$H_H \equiv T_H + V \tag{3}$$

is the high frequency oscillator Hamiltonian including the interaction between high frequency modes and low frequency modes. The subscript 'H' and 'L' represent 'high frequency modes' and 'low frequency modes' respectively. We first solve

$$H_H\Phi_a(\mathbf{Q};\mathbf{q}) = U_a(\mathbf{q})\Phi_a(\mathbf{Q};\mathbf{q}) \tag{4}$$

to get the 'potential energy surface (PES)' of low frequency modes. Then we solve

$$[T_L + U_a(\mathbf{q})]\Theta_{av}(\mathbf{q}) = E_{av}\Theta_{av}(\mathbf{q}) \tag{5}$$

to obtain the total wavefunction

$$\Psi_{av}(\mathbf{Q},\mathbf{q}) = \Phi_a(\mathbf{Q};\mathbf{q})\Theta_{av}(\mathbf{q}) \tag{6}$$

Here semicolon means that q is regarded as a parameter in $\Phi_a(\mathbf{Q};\mathbf{q})$ The performance for the adiabatic approximation has been tested and is shown to be acceptable [31]. In Eqs. (4)–(6), a denotes the quantum state of the high frequency modes **Q**, while v represents the quantum states of the low frequency modes **q**.

Notice that

$$V(\mathbf{Q},\mathbf{q}) = V_H(\mathbf{Q}) + V_L(\mathbf{q}) + V_{int}(\mathbf{Q},\mathbf{q}) \tag{7}$$

$$V_H(\mathbf{Q}) = \sum_I \frac{1}{2}\omega_I^2 Q_I^2 + \frac{1}{6}\sum_{IJK} V_{IJK}Q_IQ_JQ_K + \cdots \tag{8}$$

$$V_L(\mathbf{q}) = \sum_i \frac{1}{2}\omega_i^2 q_i^2 + \frac{1}{6}\sum_{ijk} V_{ijk}q_iq_jq_k + \cdots \tag{9}$$

$$V_{int}(\mathbf{Q},\mathbf{q}) = \frac{1}{2}\sum_{Iji} V_{Iji}Q_Iq_jq_i + \frac{1}{2}\sum_{Iij} V_{Iij}Q_Iq_iq_j + \cdots \tag{10}$$

V_{ijk} is the anharmonic expansion coefficients of the PES; for example,

$$V_{Iji} \equiv \left(\frac{\partial^3 V}{\partial Q_I \partial Q_J \partial q_i}\right)_0 \tag{11}$$

Using the same treatment in the internal conversion process [32], in the adiabatic approximation the IVR rate for $a \to b$ can be expressed as [8,31]

$$W^{(l)}_{b\leftarrow av} = \frac{2\pi}{\hbar}\sum_u \left|\left\langle \Theta_{bu}\right| -\hbar\omega_l \left\langle \Phi_b\left|\frac{\partial}{\partial q_l}\right|\Phi_a\right\rangle \left|\frac{\partial\Theta_{av}}{\partial q_l}\right\rangle\right|^2 D(E_{av}-E_{bu}) \tag{12}$$

$$W_{b\leftarrow av} = \sum_l W^{(l)}_{b\leftarrow av} \tag{13}$$

where

$$\left\langle \Phi_b\left|\frac{\partial}{\partial q_l}\right|\Phi_a\right\rangle = \frac{\left\langle \Phi_b\left|\frac{\partial V}{\partial q_l}\right|\Phi_a\right\rangle}{U_a(\mathbf{Q}) - U_b(\mathbf{Q})} \approx \frac{\left\langle \Phi^0_b\left|\frac{\partial V}{\partial q_l}\right|\Phi^0_a\right\rangle}{U^0_a - U^0_b} \tag{14}$$

and D(Eav−Ebu) denotes the line-shape function. This IVR theory has recently been applied to compare with the experimental data of IVR for the two N–H vibrational modes of isolated aniline reported by Ebata et al. [19,20]. The agreement is acceptable in [33].

3. Calculated results-$(H_2O)_2H^+$ and $(H_2O)_2$

3.1. The isotope effect in IVR of $(H_2O)_2H^+$

We now consider the application of the adiabatic approximation model of IVR to calculate the IVR rates of the hydrogen-bonded water dimer $(H_2O)_2H^+$ and its deuterated and tritiated species. We select the MP2 method and 6-311++G(d, p) basis set to optimize the geometry of all the water clusters using GAUSSIAN 09 program [34], and then calculate the anharmonic coupling parameters. The optimized structure of $(H_2O)_2H^+$ is shown in Figure 1.

The vibrational modes of $(H_2O)_2H^+$ are shown in Figure S1 in supplementary material and the rates of IVR for the O–H related modes that play the important role for the dissociation of $(H_2O)_2H^+$ to H_2O and H_3O^+ will be presented.

The frequencies of normal modes in $(H_2O)_2H^+$, $(H_2O)_2D^+$, and $(H_2O)_2T^+$, which are related to the motions of the bridged hydrogen, deuterium and tritium atoms, obviously decrease due to mass increase. Overall vibrational redistribution rates for high frequency modes 12–15 of $(H_2O)_2H^+$, $(H_2O)_2D^+$ and $(H_2O)_2T^+$ are calculated according to Eq. (13) and listed in Table 1. From this table, we find that the IVR rates slow down with the increase of the atomic weight of the bridged atom, that is, the IVR rates of the O–H modes in the $(H_2O)_2H^+$ are faster than those in the $(H_2O)_2D^+$ and $(H_2O)_2T^+$ species. This phenomenon is often referred to as 'blocking effect', for which the bridge hydrogen atom is replaced by deuterium and tritium atom. The decrease of frequency means there must be more quanta of vibrational modes to accept energy, which lowers the vibrational transition rate. For example, for vibrational mode 13, the IVR rate for the H-species is 1.96 ps, while for the D-species and T-species, the rates are 5.20 and 7.46 ps, respectively.

Next we consider other deuterated species of $(H_2O)_2H^+$ which are listed in Table 2. Let us first consider $(H_2O{\cdot}H{\cdot}HOD)^+$ and $(H_2O{\cdot}D{\cdot}HOD)^+$. We can see that the IVR rates of any O–H mode in the H bridged species are faster than those in the D bridged species. On the contrary the IVR rate of the O–D mode is faster in the D bridged species. Similarly we compare the IVR rates in $(D_2O{\cdot}H{\cdot}D_2O)^+$ and $(D_2O{\cdot}D{\cdot}D_2O)^+$; the IVR rates of the four O–D modes in the H-species are faster than those in the D-species except mode 12. Finally we compare the IVR rates in $(HOD{\cdot}H{\cdot}HOD)^+$ and $(HOD{\cdot}D{\cdot}HOD)^+$ except mode 12. In conclusion, the IVR rates of the O–H modes in the H-species almost remain to be faster than those in the D-species.

3.2. The vibrational redistribution of water clusters $(H_2O)_n$

The optimized structure of water dimer is shown in Figure 2. The point group of water dimer is C_S. There are 8 symmetric

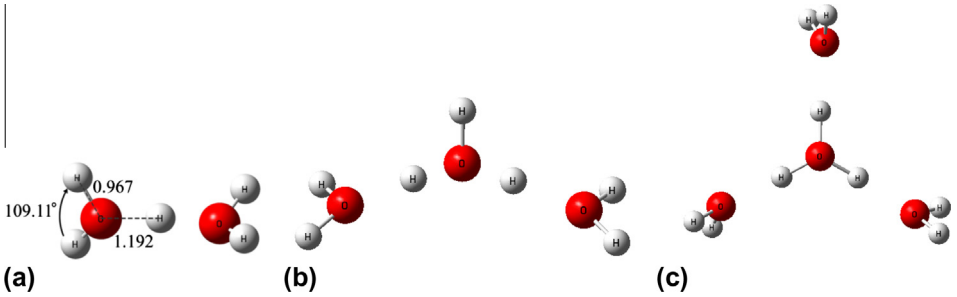

Figure 1. Equilibrium geometry of $(H_2O)_2H^+$, $(H_2O)_3H^+$ and $(H_2O)_4H^+$.

Table 1
The overall IVR rates of $(H_2O)_2H^+$, $(H_2O)_2D^+$and $(H_2O)_2T^+$.

	$(H_2O)_2H^+$			$(H_2O)_2D^+$			$(H_2O)_2T^+$		
Mode	ω (cm^{-1})	Rate (s^{-1})	τ (ps)	ω (cm^{-1})	Rate (s^{-1})	τ (ps)	ω (cm^{-1})	Rate (s^{-1})	τ (ps)
12	3790	1.89×10^{11}	5.30	3789	7.64×10^{10}	13.1	3789	4.55×10^{10}	22.0
13	3798	5.11×10^{11}	1.96	3798	1.92×10^{11}	5.20	3798	1.34×10^{11}	7.46
14	3893	4.65×10^{10}	21.5	3893	1.34×10^{10}	74.7	3893	9.59×10^{9}	104
15	3893	8.87×10^{10}	11.3	3893	1.19×10^{10}	84.0	3893	8.34×10^{9}	120

Table 2
IVR rates of deuterated $(H_2O)_2H^+$, $(H_2O)_3H^+$ and $(H_2O)_4H^+$.

Mode	Frequency (cm^{-1})	Rate(s^{-1})	Lifetime (ps)	Mode	Frequency (cm^{-1})	Rate(s^{-1})	Lifetime (ps)
1. $(H_2O{\cdot}D{\cdot}H_2O)^+$				*2. $(H_2O{\cdot}H{\cdot}HOD)^+$*			
12	3789	7.64×10^{10}	13.1	12	2792	4.17×10^{10}	24.0
13	3798	1.92×10^{11}	5.20	13	3794	5.64×10^{11}	1.77
14	3893	1.34×10^{10}	74.7	14	3849	1.04×10^{11}	9.64
15	3893	1.19×10^{10}	84.0	15	3893	5.19×10^{10}	19.3
3. $(H_2O{\cdot}H{\cdot}D_2O)^+$				*4. $(HOD{\cdot}H{\cdot}HOD)^+$*			
12	2735	7.17×10^{11}	1.39	12	2789	3.08×10^{10}	32.4
13	2859	8.85×10^{10}	11.3	13	2795	2.69×10^{11}	3.72
14	3794	5.57×10^{11}	1.79	14	3847	3.80×10^{10}	26.3
15	3893	5.25×10^{10}	19.0	15	3851	5.93×10^{10}	16.9
5. $(H_2O{\cdot}D{\cdot}HOD)^{+\cdot}$				*6. $(H_2O{\cdot}D{\cdot}D_2O)^+$*			
12	2791	1.40×10^{11}	7.17	12	2734	4.27×10^{11}	2.34
13	3793	2.29×10^{11}	4.37	13	2859	3.47×10^{10}	28.8
14	3849	2.95×10^{10}	34.0	14	3793	2.14×10^{11}	4.66
15	3893	2.49×10^{9}	402	15	3893	2.17×10^{9}	460
7. $(HOD{\cdot}D{\cdot}HOD)^+$				*8. $(DOH{\cdot}D{\cdot}HOD)^+$*			
12	2788	9.98×10^{10}	10.0	12	2790	1.18×10^{11}	8.44
13	2794	1.10×10^{11}	9.07	13	2798	1.37×10^{11}	7.31
14	3847	5.67×10^{9}	176	14	3842	1.82×10^{10}	54.9
15	3851	2.51×10^{10}	40.0	15	3850	3.95×10^{10}	25.3
9. $(D_2O{\cdot}H{\cdot}D_2O)^+$				10. $(D_2O{\cdot}D{\cdot}D_2O)^+$			
12	2730	2.07×10^{11}	4.82	12	2729	2.32×10^{11}	4.32
13	2740	8.89×10^{11}	1.13	13	2740	7.15×10^{11}	1.40
14	2859	6.51×10^{10}	15.4	14	2859	2.12×10^{10}	47.1
15	2859	1.59×10^{11}	6.28	15	2859	3.74×10^{10}	26.7
11. $(H_2O)_3H^+$				*12. $(H_2O)_4H^+$*			
20	3844	1.44×10^{11}	6.95	28	3852	2.22×10^{11}	4.51
21	3845	2.31×10^{11}	4.33	29	3852	1.79×10^{11}	5.58
22	3863	2.08×10^{11}	4.80	30	3853	2.88×10^{11}	3.62
23	3951	2.52×10^{10}	39.7	31	3958	3.20×10^{10}	31.2
24	3951	2.61×10^{10}	38.4	32	3958	3.19×10^{10}	31.4
				33	3959	2.11×10^{10}	47.5

modes and 4 anti-symmetric modes. The IVR rates of water dimer $(H_2O)_2$ are given in Table 3 and Table 4. Table 3 gives the overall IVR rates of six intramolecular modes which seem to correlate with the energy gap to be relaxed into low frequency modes, which calculated according to Eq. (12). Table 4 gives the important detailed vibrational redistribution rates, that is, the fastest IVR paths of water dimer. From these tables, we know that the fastest vibrational redistribution rate is $1.94 \times 10^{11}\ s^{-1}$ for the mode 9. An important feature is that the detailed redistribution rates such as $W_{11,8,8}$, $W_{10,7,7}$, $W_{9,8,8}$,

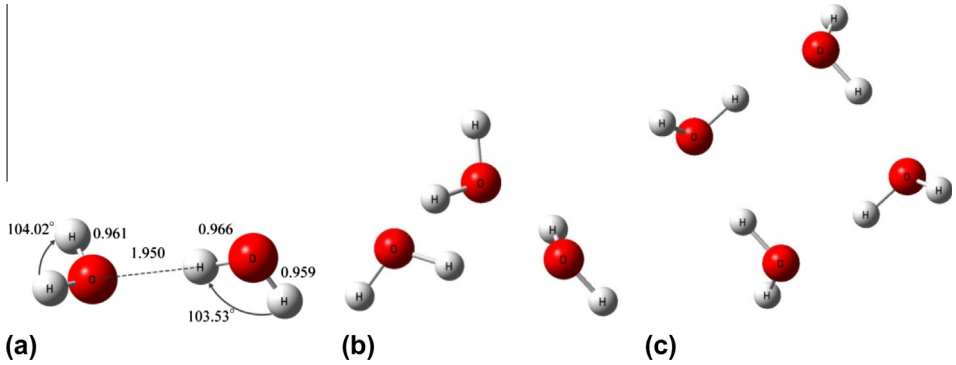

Figure 2. Equilibrium geometry of $(H_2O)_2$, $(H_2O)_3$ and $(H_2O)_4$.

Table 3
The overall IVR rates of $(H_2O)_2$, $(H_2O)_3$ and $(H_2O)_4$.

Mode	Frequency (cm^{-1})	Rate (s^{-1})	Lifetime (ps)
$(H_2O)_2$			
7	1639	2.20×10^9	454
8	1664	3.52×10^9	284
9	3807	1.94×10^{11}	5.15
10	3877	3.16×10^{10}	31.6
11	3974	8.82×10^9	113
12	3990	1.77×10^9	566
$(H_2O)_3$			
16	3688	5.22×10^{11}	1.92
17	3739	1.10×10^{11}	9.05
18	3747	1.59×10^{11}	6.29
19	3961	1.99×10^{10}	50.14
20	3964	2.14×10^{10}	46.69
21	3965	2.04×10^{10}	49.01
$(H_2O)_4$			
23	3526	2.55×10^{12}	0.392
24	3608	4.77×10^{11}	2.10
25	3608	4.77×10^{11}	2.10
26	3644	4.13×10^{11}	2.42
27	3953	1.65×10^{10}	60.6
28	3955	1.64×10^{10}	61.0
29	3955	1.64×10^{10}	61.0
30	3955	2.15×10^{10}	46.6
23	3526	2.55×10^{12}	0.392

Table 4
Vibrational relaxation paths of $(H_2O)_2$. Accepting Energy = $\omega_n - \omega_l - \omega_k$.

I	l	k	R_{nlk}	Accpt. energy (cm^{-1})	Rate (s^{-1})
7	6	6	0.054	301	2.20×10^9
8	6	6	0.027	325	3.42×10^9
9	8	8	0.063	479	1.86×10^{11}
10	7	7	0.065	599	3.16×10^{10}
11	8	8	0.015	646	6.08×10^9
12	8	3	0.104	2149	8.51×10^8

$W_{8,6,6}$, and $W_{7,6,6}$ play important roles in the vibrational redistribution of $(H_2O)_2$, which indicates the low frequency modes tend to accept two quanta energy from the high frequency modes.

The calculated results of IVR for other common water clusters $(H_2O)_n$ and $(H_2O)_nH^+$ where $n = 3$ and 4 are also shown in Table 3 and Table 2. As can be seen from these results, the IVR rates in most cases do increase with the size of cluster (maybe slowly). This indicates that it may be possible to regard the liquid water to consist of various size of clusters $n = 2$–4 or 5. For the case of $(H_2O)_3$ and $(H_2O)_3H^+$, the IVR rates of the first three O–H modes are much faster than the remaining ones. On the other hand, for the case of $(H_2O)_4$ and $(H_2O)_4H^+$, while there are four fast OH modes in $(H_2O)_4$. The fastest IVR rates of the OH modes in $(H_2O)_n$ are usually much faster than those of the corresponding $(H_2O)_nH^+$. For the IVR rates of $(H_2O)_n$ with $n = 2$, 3, 4 shown in Table 3, we compare the IVR rates of the lowest O–H modes, 3807 cm^{-1} for $n = 2$, 3688 cm^{-1} for $n = 3$ and 3526 cm^{-1} for $n = 4$. We can see their IVR rates are, respectively, 5.15 ps, 1.91 ps and 0.39 ps. There exists approximately a general tendency, that is, the IVR rates vary with their O–H vibrational frequencies.

From the results of our calculated IVR rates of $(H_2O)_n$, we can suggest that in the bulk water the size of water clusters must be $n \geqslant 3$.

4. Discussion

4.1. Dipole vibrational–vibrational energy transfer

The vibrational energy transfer can also take place in a cluster or between molecules through dipole–dipole interaction.[35] In this Letter only the resonance energy transfer case is considered; the non-resonance case can also be treated [32,35].

The vibrational energy transfer may take place between O–H stretching modes or O–D stretching modes in $(HOD)_2H^+$. We define the vibrational energy transfers from the 'Donor' part to the 'Acceptor' part. According to Ref. [12,35], the transfer rate by dipole–dipole interaction can be presented as

$$W_{\mathrm{VET}} = \frac{2\pi}{\hbar}\sum_{v,u}\rho_{nv}^{(b)}|\langle nv|H'_{\mathrm{DA}}|n'v'\rangle|^2 D(E_{n'v'} - E_{nv}) \tag{15}$$

where $\rho_{nv}^{(b)}$ is the distribution function, and

$$H'_{\mathrm{DA}} = \frac{|\vec{\mu}_{\mathrm{D}}^{l}||\vec{\mu}_{\mathrm{A}}^{k}|}{4\pi\varepsilon\varepsilon_0 R_{\mathrm{DA}}^3}\Omega \tag{16}$$

$$\Omega = \cos\theta_{\mathrm{DA}}^{lk} - 3\cos\theta_{\mathrm{D}}^{l}\cos\theta_{\mathrm{A}}^{k} \tag{17}$$

$$D(E_{n'v'} - E_{nv}) = \frac{1}{\pi}\frac{\hbar\gamma}{(E_{n'v'} - E_{nv})^2 + \hbar^2\gamma^2} \tag{18}$$

The dipoles $\vec{\mu}_{\mathrm{D}}^{l}$ and $\vec{\mu}_{\mathrm{A}}^{k}$ in Eq. (16) are defined as

$$\vec{\mu}_{\mathrm{D}}^{l} = \left(\frac{\partial\vec{\mu}_{\mathrm{D}}}{\partial Q_{\mathrm{D},l}}\right)_0 Q_{\mathrm{D},l};\ \vec{\mu}_{\mathrm{A}}^{l} = \left(\frac{\partial\vec{\mu}_{\mathrm{A}}}{\partial Q_{\mathrm{A},k}}\right)_0 Q_{\mathrm{A},k}. \tag{19}$$

$\theta_{\mathrm{DA}}^{lk}$ is the angle between $\vec{\mu}_{\mathrm{D}}^{l}$ and $\vec{\mu}_{\mathrm{A}}^{k}$, and θ_{D}^{l}, θ_{A}^{k} represent the angles between $\vec{\mu}_{\mathrm{D}}^{l}$, $\vec{\mu}_{\mathrm{A}}^{k}$ and $\vec{R}_{\mathrm{DA}}$, respectively. For the transition $(n_{\mathrm{D}}^{l} = 1, n_{\mathrm{A}}^{k} = 0) \rightarrow (n_{\mathrm{D}}^{l} = 0, n_{\mathrm{A}}^{k} = 1)$, Eq. (15) can be rewritten as

$$W_{\mathrm{VET}} = \frac{2\pi}{\hbar^2}\frac{\Omega^2}{(4\pi\varepsilon\varepsilon_0)^2 R_{\mathrm{DA}}^6}\left|\left(\frac{\partial\vec{\mu}_{\mathrm{D}}}{\partial Q_{\mathrm{D},l}}\right)_0\right|^2\left|\left(\frac{\partial\vec{\mu}_{\mathrm{A}}}{\partial Q_{\mathrm{A},k}}\right)_0\right|^2 \times \frac{\hbar^2}{4\omega_{\mathrm{D},l}\omega_{\mathrm{A},k}}D(\omega_{\mathrm{D},l} - \omega_{\mathrm{A},k}). \tag{20}$$

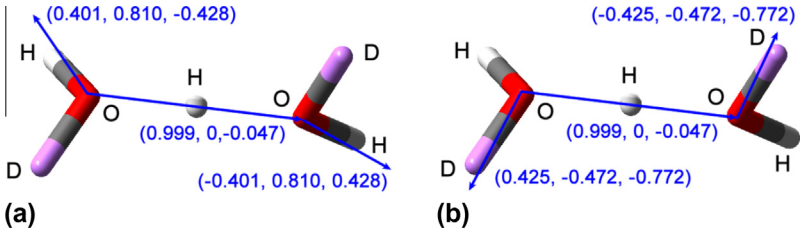

Figure 3. Vibrational energy transfer between (a) OH-OH and (b) OD-OD in $(HOD)_2H^+$.

To calculate the vibrational energy transfer between O–H bond stretching modes and O–D bond stretching modes, we first optimize the equilibrium structure of $(HOD)_2H^+$. Then we calculate the dipole derivatives of O–H bond stretching mode and O–D bond stretching mode in monomer HOD. The frequencies of OH and OD stretching modes are 3946 cm^{-1} and 2864 cm^{-1}, respectively. We use O–O bond length in $(HOD)_2H^+$ for the distance R_{DA}, which is 2.38 Å. According Eq. (17), Ω_{OH} and Ω_{OD} are 0.843 and −0.101 respectively. The resonance energy transfers taking place in $(HOD)_2H^+$ and the dipole derivatives localizing on each mode in the dimer $(HOD)_2H^+$ are shown in Figure 3. The numbers in Figure 3 represent the unit vectors of OH, OD and OO, which is used to calculate Ω_{OH} and Ω_{OD}. In the resonance case, $E_{bu} \approx E_{av}$ Then Lorentzian function in Eq. (18) can be approximately derived as

$$D(E_{bu} - E_{av}) = \frac{1}{\pi h \gamma} \tag{21}$$

Set the dephasing parameter $\gamma = 10^{12}\ s^{-1}$, and according to Eqs. (15)–(21), The vibrational energy transfer rates between OH stretching modes and OD stretching modes in $(HOD)_2H^+$ are $1.24 \times 10^{11}\ s^{-1}$ and $7.61 \times 10^{8}\ s^{-1}$, respectively.

In photochemistry, the electronic excitation energy transfer between the excited donor molecule D^* and un-excited acceptor molecule A is usually described by the Förster theory using the dipole–dipole interaction which is in turn expressed in terms of the spectral overlap between the normalized fluorescence spectra of D^* and the absorption spectra of A. However, it should be noted that in this case to describe the electronic states of D^* and A no configurational interactions have been considered, which resulted in the Coulomb interaction and exchange interaction. Furthermore, the exchange interaction is ignored and the Coulomb interaction is replaced by the multipole expansion and only first non-vanishing dipole–dipole interaction is retained.

The vibrational energy transfer can also take place in cluster or between molecules. Here again only the dipole–dipole interaction is employed. In this Letter only the resonance energy transfer case is considered; the non-resonance case can also be treated [31,35]. In the non-resonance case the 'Franck–Condon' factor $|\langle\Theta_{bu}|\Theta_{av}\rangle|^2$ of Eq. (15) should be properly treated.

4.2. IVR and the RRKM theory

The RRKM rate constant for an isolated molecule with energy E can be expressed as

$$k(E) = \frac{1}{h}\frac{W^{\neq}(E - E_0^{\neq})}{\rho(E)} \tag{22}$$

where $E_0^{\neq}$ denotes the activation energy, $W^{\neq}(E - E_0^{\neq})$, the total number of states of the activated complex and $\rho(E)$, the density of states of the reactant. The dissociation rate of $(H_2O)_2H^+$ was calculated by using the anharmonic RRKM theory [25].

The activation energy of the variational TS is obtained to be 30.95 kcal/mol for the dissociation of $(H_2O)_2H^+$ in the paper by Song et al., [25] which corresponds to 10825 cm^{-1}. We calculate the vibrational redistribution rate from $n = 3$ to $n = 2$ and from $n = 2$ to $n = 1$. From the Eq. (12) we can derive that approximately

$$W(n \to n-1) = nW(1 \to 0) \tag{23}$$

From Eq. (23), the IVR rates from $n = 3$ to $n = 2$ are $5.66 \times 10^{11}\ s^{-1}$, $1.54 \times 10^{12}\ s^{-1}$, $1.39 \times 10^{11}\ s^{-1}$ and $2.66 \times 10^{11}\ s^{-1}$ corresponding to modes 9–12, respectively. Now we shall examine the validity of the RRKM theory by comparing the IVR rates and the dissociation rate in RRKM method. Song et al. [25] have applied the anharmonic RRKM theory to calculate the dissociation rate of $(H_2O)_2H^+$. Near the dissociation threshold of $(H_2O)_2H^+$, the dissociation rate calculated in microcanonical ensemble is about $4.34 \times 10^{6}\ s^{-1}$. This is much slower than the IVR rates listed above. Thus in this case it is valid to use the RRKM theory to calculate the decomposition of $(H_2O)_2H^+$.

Yao et al. have calculated the dissociation rate of water dimer with the anharmonic RRKM method [27]. Comparing the IVR rates (see Table 3) and the dissociation rate of $(H_2O)_2$, $1.95 \times 10^{11}\ s^{-1}$ [27], we can see that the transition state theory is not valid. In this case the quantum mechanical vibrational predissociation theory should be employed [36,37].

In conclusion, to check the validity of the RRKM theory for unimolecular decompositions of these water clusters, we find that for the dissociation of $(H_2O)_2$, the RRKM theory is not valid to be employed, and for the case of $(H_2O)_2H^+$, the RRKM theory holds to a considerable excitation energy range.

5. Summary

Recently vibration dynamics of liquid water and surface water has attracted considerable attention experimentally. To study this vibration dynamics the anharmonic coupling potentials are required which have become available only recently. In this Letter we use this information to calculate the vibrational redistribution in water clusters $(H_2O)_n$ and $(H_2O)_nH^+$ with $n = 2,3$ and 4. The IVR rate does exhibit its increase with the size of cluster and reaches the values of liquid water at $n \geqslant 3$. For $(H_2O)_3$ and $(H_2O)_4$; their fastest IVR rates are in the same order of magnitudes as these of bulk and surface water [1]. This indicates that in the bulk water or surface water, the water clusters of $n \geqslant 3$ exist and although their structures may change, the changed rates must be slower than picoseconds.

The isotope effect on IVR is also investigated. We make use of $(H_2O{\cdot}H{\cdot}H_2O)^+$ to $(H_2O{\cdot}D{\cdot}H_2O)^+$ and $(H_2O{\cdot}T{\cdot}H_2O)^+$ to study the blocking effect of IVR, that is, the IVR rate decreases with H^+, D^+ and T^+ in the cluster. Making use of $(HOD{\cdot}H{\cdot}HOD)^+$ we study the resonance energy transfer between O–H and O–H, and O–D and O–D in the cluster and find the vibrational energy transfer rates to be in the range of $1.24 \times 10^{11}\ s^{-1}$–$7.61 \times 10^{8}\ s^{-1}$, sensitively depending on the relative orientation of the vibrational dipole moments and relative distance.

We make use of the calculated IVR rates in $(H_2O)_2$ and $(H_2O)_2H^+$ to check the validity of the use of the RRKM theory for the dissociation of $(H_2O)_2$ and $(H_2O)_2H^+$. We find that the RRKM theory can be applied to the case of $(H_2O)_2H^+$ but not to $(H_2O)_2$.

Acknowledgment

This work was supported by the National Science Council of Taiwan and National Chiao-Tung University.

Appendix A. Supplementary data

Supplementary data associated with this article can be found, in the online version, at http://dx.doi.org/10.1016/j.cplett.2013.09.019.

References

[1] J.A. McGuire, Y.R. Shen, Science 313 (2006) 1945.
[2] M.L. Cowan, B.D. Bruner, N. Huse, J.R. Dwyer, B. Chugh, E.T.J. Nibbering, T. Elsaesser, R.J.D. Miller, Nature 434 (2005) 199.
[3] A.J. Lock, H.J. Bakker, J. Chem. Phys. 117 (2002) 1708.
[4] A.J. Lock, S. Woutersen, H.J. Bakker, J. Phys. Chem. A 105 (2001) 1238.
[5] N. Huse, S. Ashihara, E.T.J. Nibbering, T. Elsaesser, Chem. Phys. Lett. 404 (2005) 389.
[6] T. Elsaesser, W. Kaiser, Annu. Rev. Phys. Chem. 42 (1991) 83.
[7] J.P. Maier, A. Seilmeier, A. Laubereau, W. Kaiser, Chem. Phys. Lett. 46 (1977) 527.
[8] S.H. Lin, J. Chem. Phys. 65 (1976) 1053.
[9] D.W. Oxtoby, Annu. Rev. Phys. Chem. 32 (1981) 77.
[10] S.A. Egorov, J.L. Skinner, J. Chem. Phys. 105 (1996) 7047.
[11] S.A. Egorov, J.L. Skinner, J. Chem. Phys. 105 (1996) 10153.
[12] M. Hayashi, Y. Shiu, K.K. Liang, S.H. Lin, Y.R. Shen, J. Phys. Chem. A 111 (2007) 9062.
[13] M. Yang, F. Li, J.L. Skinner, J. Chem. Phys. 135 (2011) 164505.
[14] A. Bastida, J. Zuniga, A. Requena, B. Miguel, J. Chem. Phys. 136 (2012) 234507.
[15] R. Rey, K.B. Møller, J.T. Hynes, Chem. Rev. 104 (2004) 1915.
[16] T. Yagasaki, J. Ono, S. Saito, J. Chem. Phys. 131 (2009) 164511.
[17] L.C. Ch ng, A.K. Samanta, G. Czakó, J.M. Bowman, H. Reisler, J. Am. Chem. Soc. 134 (2012) 15430.
[18] Y. Yamada, Y. Katsumoto, T. Ebata, Phys. Chem. Chem. Phys. 9 (2007) 1170.
[19] Y. Yamada, J. Okano, N. Mikami, T. Ebata, Chem. Phys. Lett. 432 (2006) 421.
[20] Y. Yamada, J. Okano, N. Mikami, T. Ebata, J. Chem. Phys. 123 (2005) 124316.
[21] O.K. Rice, H.C. Ramsperger, J. Am. Chem. Soc. 49 (1927) 1617.
[22] L.S. Kassel, J. Phys. Chem. 32 (1927) 225.
[23] H. Eyring, J. Chem. Phys. 3 (1935) 107.
[24] R. Marcus, J. Chem. Phys. 20 (1952) 359.
[25] D. Song, H. Su, F. Kong, S.H. Lin, J. Phys. Chem. A 114 (2010) 10217.
[26] L. Yao, A.M. Mebel, S.H. Lin, J. Phys. Chem. A 113 (2009) 14664.
[27] L. Yao, R.X. He, A.M. Mebel, S.H. Lin, Chem. Phys. Lett. 470 (2009) 210.
[28] L. Yao, A.M. Mebel, H.F. Lu, H.J. Neusser, S.H. Lin, J. Phys. Chem. A 111 (2007) 6722.
[29] V. Barone, J. Chem. Phys. 122 (2005) 14108.
[30] V. Barone, J. Chem. Phys. 120 (2004) 3059.
[31] Z.D. Qian, X.G. Zhang, X.W. Li, H. Kono, S.H. Lin, Mol. Phys. 47 (1982) 713.
[32] S.H. Lin, J. Chem. Phys. 44 (1966) 3759.
[33] N. Yingli, L. Chinkai, Y. Ling, Y. Jianguo, H. Rongxing, P. Ran, Z. Chaoyuan, H. Michitoshi, L.S. Hsien, Prog. Chem. 24 (2012) 928.
[34] MJ Frisch et al., Gaussian 09, Revision E.01, Gaussian, Inc., 2009.
[35] A. Blumen, S.H. Lin, J. Manz, J. Chem. Phys. 69 (1978) 881.
[36] R. Chang, J.C. Jiang, P.J. Hsieh, H.C. Chang, S.H. Lin, J. Chin. Chem. Soc. 46 (1999) 417.
[37] S.H. Lin, A. Boeglin, Y. Fujimura, B. Fain, Chem. Phys. Lett. 145 (1988) 334.